Cell, Vol. 105, 445–457, May 18, 2001, Copyright ©2001 by Cell Press

Securin Is Required for Chromosomal Stability in Human Cells

Prasad V. Jallepalli,[1] Irene C. Waizenegger,[3] Fred Bunz,[1] Sabine Langer,[4] Michael R. Speicher,[4] Jan-Michael Peters,[3] Kenneth W. Kinzler,[1] Bert Vogelstein,[1,2] and Christoph Lengauer[1,5]

[1]The Johns Hopkins Oncology Center
[2]Howard Hughes Medical Institute
1650 Orleans Street
Baltimore, Maryland 21231
[3]Research Institute of Molecular Pathology
Vienna 1030
Austria
[4]Institute of Anthropology and Human Genetics
University of Munich
Munich 80333
Germany

Summary

Abnormalities of chromosome number are the most common genetic aberrations in cancer. The mechanisms regulating the fidelity of mitotic chromosome transmission in mammalian cells are therefore of great interest. Here we show that human cells without an *hSecurin* gene lose chromosomes at a high frequency. This loss was linked to abnormal anaphases during which cells underwent repetitive unsuccessful attempts to segregate their chromosomes. The abnormal mitoses were associated with biochemical defects in the activation of separin, the sister-separating protease, rendering it unable to cleave the cohesin subunit Scc1 efficiently. These results illuminate the function of mammalian securin and show that it is essential for the maintenance of euploidy.

Introduction

Genetic instability is now widely recognized as an essential factor in the evolution of cancer (Loeb, 1991; Lengauer et al., 1998). In the vast majority of solid tumors, this instability appears to involve gains and losses of whole chromosomes or large parts thereof, leading to aneuploidy (Lengauer et al., 1997; Duesberg et al., 1999). Recent evidence suggests that this form of chromosomal instability (CIN) is in some cases associated with alterations in a cell cycle checkpoint that monitors the integrity of the spindle apparatus, a structure critical for proper bipolar segregation of duplicated sister chromatids at mitosis (Cahill et al., 1999). A small fraction of CIN cancers are associated with dominant mutations in the human homolog of the yeast spindle checkpoint gene *BUB1* (Cahill et al., 1998; Imai et al., 1999; Gemma et al., 2000). Likewise, mutations in the mouse *BUB1* gene have been shown to disrupt the mitotic spindle checkpoint (Taylor and McKeon, 1997; Lee et al., 1999). Efforts to study the mitotic spindle checkpoint pathway through genetic approaches have been hampered by the extremely early embryonic lethality of mice homozygously deleted for *MAD2* and *BUB3*, preventing the evaluation of chromosome loss rates in proliferating somatic cells (Dobles et al., 2000; Kalitsis et al., 2000). However, recent evidence suggests that disruption of a single *MAD2* allele can result in a modest increase in chromosomal instability associated with premature anaphase entry (Michel et al., 2001).

Intensive efforts to dissect the mitotic spindle checkpoint biochemically have elucidated a general mechanism by which BUB1 and other checkpoint proteins arrest mitotic progression in response to spindle damage (reviewed in Amon, 1999; Gardner and Burke, 2000). Specific MAD and BUB proteins are localized to the kinetochores of chromosomes that are unattached to the spindle apparatus (Chen et al., 1996; Li and Benezra, 1996; Taylor et al., 1998; Martinez-Exposito et al., 1999), suggesting that they trigger the checkpoint in cells exposed to microtubule inhibitors or in cells with spontaneously lagging chromosomes. At the biochemical level, the BUB and MAD protein kinase cascade ultimately impinges on a large multiprotein assembly known as the anaphase-promoting complex (APC) that appears to be the master regulator of chromosome segregation and mitotic exit in all eukaryotic cells (for reviews see King et al., 1996; Morgan, 1999; Peters, 1999). Although the mechanisms regulating APC activity are not yet completely understood, it seems clear that at least one outcome of activation of the MAD/BUB pathway is the association of MAD2 with the APC and its accessory factor Cdc20 (Fang et al., 1998). This association inhibits the intrinsic ubiquitinating activity of the APC^{Cdc20} complex, thereby preventing the degradation of securin and later of cyclin B. Activation of the checkpoint thereby delays anaphase and exit from mitosis until all sister chromatids have established bipolar attachments to the spindle apparatus.

The securin proteins are key substrates of the APC pathway and comprise an evolutionarily divergent class of anaphase inhibitors. Members of the securin family include the Pds1 and Cut2 proteins in budding and fission yeast, respectively, the vertebrate pituitary-tumor transforming gene (PTTG or vSecurin) proteins, and the Pimples protein in *Drosophila* (Cohen-Fix et al., 1996; Funabiki et al., 1996b; Stratmann and Lehner, 1996; Zou et al., 1999). The securins form tight complexes with a well-conserved family of proteins, the "sister-separating" proteases that have been termed separins (reviewed by Nasmyth et al., 2000; Yanagida, 2000). Securin degradation appears to be essential for sister chromatid separation, as expression of nondegradable securins blocks chromosome segregation in both budding and fission yeasts and in animal cells (Cohen-Fix et al., 1996; Funabiki et al., 1996b; Zou et al., 1999; Leismann et al., 2000). Based on these and other data, current models propose that securin destruction liberates the active separin protease, allowing it to cleave proteins mediating sister chromatid cohesion, including the cohesin subunit Scc1 (Glotzer, 1999; Uhlmann et al., 1999; Nasmyth et al., 2000; Uhlmann et al., 2000; Waizenegger et al., 2000).

[5]Correspondence: lengauer@jhmi.edu

This would release tension between paired kinetochores, allowing the separated sister chromatids to migrate poleward along the mitotic spindle.

Paradoxically, there is also evidence that securin plays a positive role in promoting sister separation. In fission yeast, loss of securin is lethal and produces the same effect as loss of separin itself, i.e., a complete block to chromosome segregation and completion of mitosis (Funabiki et al., 1996a). Similarly, *Drosophila pimples* mutants fail to separate sister chromatids during mitosis 15 (Stratmann and Lehner, 1996). Close examination of *pds1* mutants in *S. cerevisiae* also demonstrates retarded anaphase entry and synthetic lethality with separin mutations (Ciosk et al., 1998), arguing that even in budding yeast, securin and separin may act synergistically rather than purely antagonistically in regulating anaphase.

As a downstream target of the mitotic spindle checkpoint, the sister chromatid separation pathway may be critically important for preventing aneuploidy in higher eukaryotes, particularly in those cells that have progressed along the multistep pathway leading to cancer (Kinzler and Vogelstein, 1996; Lengauer et al., 1998). To begin to address this issue, we chose to inactivate both copies of the gene encoding hSecurin in a karyotypically stable human colorectal cancer cell line via homologous recombination. Our results indicate that hSecurin is indeed needed for chromosomal stability in humans, as hSecurin-deficient cells exhibited high chromosome loss rates, similar to those observed in naturally occurring cancers. Moreover, there was a very clear and somewhat surprising effect of hSecurin deletion. Rather than leading to premature chromatid separation, the major effect of *hSecurin* deletion was to *retard* chromosome separation. Accordingly, we found that hSecurin was essential for the proper function and processing of the separin protease, for separin-dependent cleavage of the cohesin subunit Scc1, and for maintaining chromosomal stability in mammalian cells.

Results

Generation of Human Cells Lacking hSecurin

To evaluate hSecurin function, both copies of the *hSecurin* gene were inactivated via homologous recombination in HCT116 cells. HCT116 is a well-characterized human colorectal cancer cell line that has a stable karyotype and intact DNA damage and mitotic spindle checkpoints (Lengauer et al., 1997; Bunz et al., 1998). To obtain targeted deletions, vectors containing 5′ and 3′ elements derived from the *hSecurin* locus and an antibiotic resistance marker flanked by *loxP* sites (Figure 1A) were transfected into HCT116 cells, and the resulting antibiotic-resistant clones were screened for proper integration as described in Experimental Procedures. Successfully targeted *hSecurin*$^{+/-}$ heterozygotes were transfected with a Cre recombinase plasmid to excise the antibiotic resistance marker and then retransfected with the original targeting vectors to disrupt the remaining wild-type allele.

Genomic PCR analysis with two different sets of primers spanning the first intron and second exon of the *hSecurin* gene demonstrated homozygous deletions of these sequences in two different *hSecurin*$^{-/-}$ clones (Figure 1B). Southern blot analysis confirmed that both wild-type alleles had been inactivated through homologous recombination in these clones (Figure 1C). Antibodies to hSecurin protein were made as described in Experimental Procedures. Immunoblotting with these antibodies demonstrated a lack of detectable protein in homozygously deleted cells while their isogenic controls expressed reactive polypeptides of the expected sizes (Figure 1D). For the studies reported below, a total of three *hSecurin*$^{+/-}$ clones and two *hSecurin*$^{-/-}$ clones were tested. All cells of the same genotype behaved identically.

In culture, cells lacking hSecurin grew somewhat more slowly than wild-type cells, but the cell cycle distribution of unsynchronized cells, apoptotic fraction, and percentage of cells in mitosis were essentially identical for *hSecurin*$^{+/+}$ and *hSecurin*$^{-/-}$ clones (Figures 1E and 1F). Thus, remarkably, homozygous loss of *hSecurin* is not lethal to human cells.

Chromosomal Instability in hSecurin-Deficient Cells

To examine whether securin deficiency altered the rate of chromosome loss, *hSecurin*$^{-/-}$ cells (KO1 and KO2) and isogenic control cells (HCT116) were passaged for 20 generations and analyzed by fluorescence in situ hybridization (FISH) using chromosome-specific centromeric probes. As shown in Figure 2, two fluorescent signals per autosomal chromosome per nucleus were observed in parental cells (Figure 2A). The fraction of cells with signals more or less than the modal value of 2, which is a quantitative index of CIN (Lengauer et al., 1997), was typically 1%–4% (Figures 2F and 2G). In contrast, 17% to 32% of the *hSecurin*$^{-/-}$ cells exhibited aberrant numbers of signals per nucleus (Figures 2F and 2G; examples in Figures 2B–2D).

To confirm and extend these analyses, we employed multiplex-FISH (M-FISH) to paint entire metaphase spreads and inspect chromosomes for abnormalities of structure as well as number. M-FISH analysis was restricted to near-diploid metaphases to eliminate possible errors caused by misinterpretation of any pseudotetraploid cells arising sporadically in *hSecurin*$^{+/+}$ and *hSecurin*$^{-/-}$ cells. M-FISH karyotyping confirmed the clonal chromosome rearrangements reported previously in parental HCT116 cells (Masramon et al., 2000) and confirmed the stability of its near-diploid karyotype; only a single metaphase with any chromosome loss was observed in 20 metaphase spreads (Figure 3B). In contrast, *hSecurin*$^{-/-}$ cells contained many chromosome losses, with over 80% of metaphases exhibiting at least one chromosome loss and with individual metaphases missing as many as 21 chromosomes (Figures 3C and 3D; example in Figure 3A). There was no chromosome immune from loss (Figures 3C and 3D), and the losses occurred without an increase in structural chromosomal abnormalities, as assessed by careful analysis of the M-FISH karyotypes.

FISH analysis of interphase nuclei also demonstrated a peculiar cytological abnormality in *hSecurin*$^{-/-}$ cells: a "bud" or accessory lobe reminiscent of a micronucleus but physically attached to the main nuclear body (Figure 2B). This structure was found only rarely in control cells

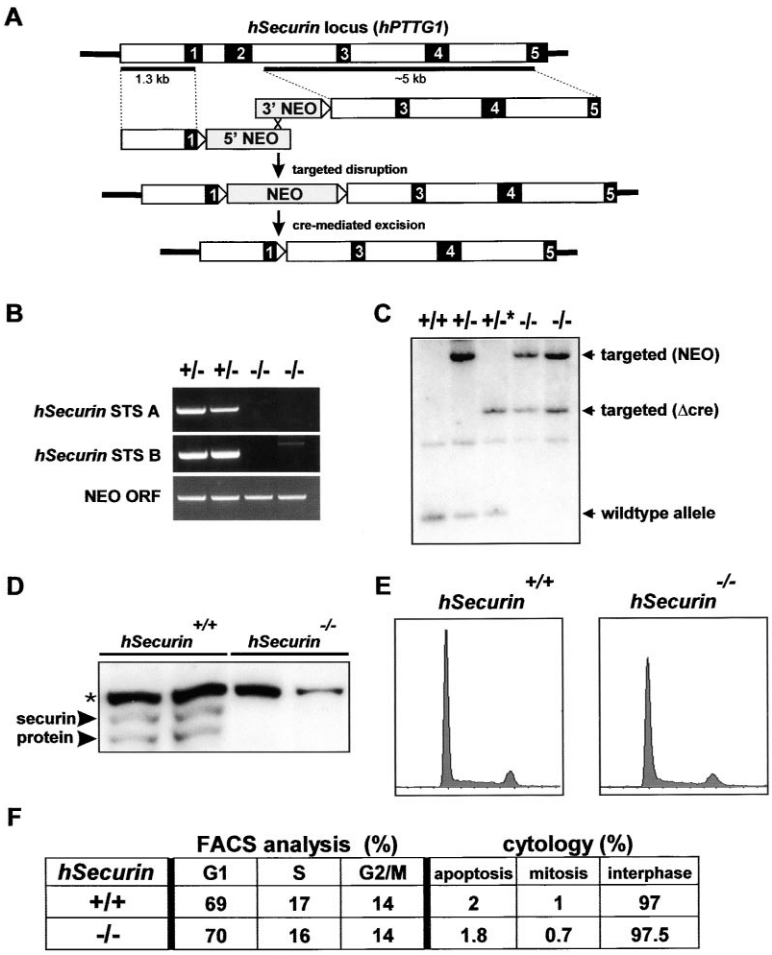

FACS analysis (%)				cytology (%)		
hSecurin	G1	S	G2/M	apoptosis	mitosis	interphase
+/+	69	17	14	2	1	97
-/-	70	16	14	1.8	0.7	97.5

Figure 1. Generation of hSecurin-Deficient Human Cells by Homologous Recombination

(A) Schematic of knockout vector design (see Experimental Procedures). Numbered black boxes refer to *hSecurin* exons.

(B) Genomic DNA was prepared from cells of the indicated genotypes and subjected to PCR analysis with two different sets of primers spanning the first intron and second exon of the *hSecurin* gene (STS A and STS B). As a control, PCR amplification of the integrated antibiotic-resistance gene (NEO ORF) was performed on the same DNA templates.

(C) Southern blot analysis confirming homozygous inactivation of the *hSecurin* locus. Genomic DNAs were digested with MseI and hybridized with a *hSecurin* probe within the 5′ homology arm depicted in (A). The lane (+/−*) corresponds to cells with one disrupted *hSecurin* allele, following cre-mediated excision of the NEO cassette.

(D) Western blotting with hSecurin antibodies. Lysates were prepared from cells of the indicated genotypes and probed with antibodies to hSecurin. Arrowheads point to the two closely spaced bands of approximately 28 kDa corresponding to phosphorylated and unphosphorylated forms of hSecurin protein. The asterisk (*) denotes a nonspecific background band that served as an internal control.

(E) Flow cytometry analysis and (F) cell cycle distribution, apoptotic fraction, and mitotic index of exponentially growing *hSecurin*$^{+/+}$ and *hSecurin*$^{-/-}$ cells.

(Figure 2G, right panel). In some cases, the chromosome-specific centromeric probes used for FISH analysis localized to this nuclear bud (Figure 2B), suggesting that it had arisen through a defect in the dynamics of whole chromosome movement. To confirm this observation, we performed FISH analysis using a probe that stained the centromeres of all chromosomes. The nuclear buds were found to contain a variable number of centromeric signals that were consistently detected even in very small buds (Figure 2E).

Sister Chromatid Cohesion Is Maintained in *hSecurin*$^{-/-}$ Cells after Spindle Damage

We first attempted to determine whether hSecurin loss resulted in chromatid separation in the presence of spindle poisons, as observed in yeast cells with Pds1 deficiency (Yamamoto et al., 1996b). Parental and *hSecurin*$^{-/-}$ cells were treated with nocodazole or colcemid and examined at various times thereafter by DAPI staining as well as by FISH using centromeric probes (Figure 4). Remarkably, we found no evidence of increased sister chromatid separation in *hSecurin*$^{-/-}$ cells, even after 18 hr of treatment with nocodazole or colcemid (Figure 4C). Thus, in contrast to budding yeast (Yamamoto et al., 1996b), human cells lacking securin still manage to arrest sister separation in the presence of spindle poisons. This unexpected finding implies that an additional mechanism of separin regulation must exist in human cells.

hSecurin$^{-/-}$ Cells Are Defective in the Execution of Anaphase

To examine normal mitotic processes in more detail, we expressed the histone H2B-GFP fusion protein (Kanda et al., 1998) in parental and *hSecurin*$^{-/-}$ cells. We were thereby able to monitor nuclear dynamics in vivo. Passage through mitosis is characterized by a series of dramatic cytological events, including rounding up of cell bodies, condensation of chromatin, dissolution of the nuclear membrane, alignment of chromosomes on the metaphase plate, and finally bipolar segregation of separated sister chromatids at anaphase. Time lapse microscopy in cells expressing histone H2B-GFP allowed us to examine these events under normal growth conditions.

The early events in mitosis, including chromatin condensation and midline congression of metaphase chromosomes, were similar in *hSecurin*$^{-/-}$ and control HCT116 cells. In control cells, the aligned chromosomes rapidly progressed into anaphase, characterized by sharp separation and bipolar segregation of sister chromatids (Figure 5A). In contrast, over a third of *hSecurin*$^{-/-}$ cells failed to separate their metaphase chromosomes appropriately. In many cases, the GFP-stained nuclear mate-

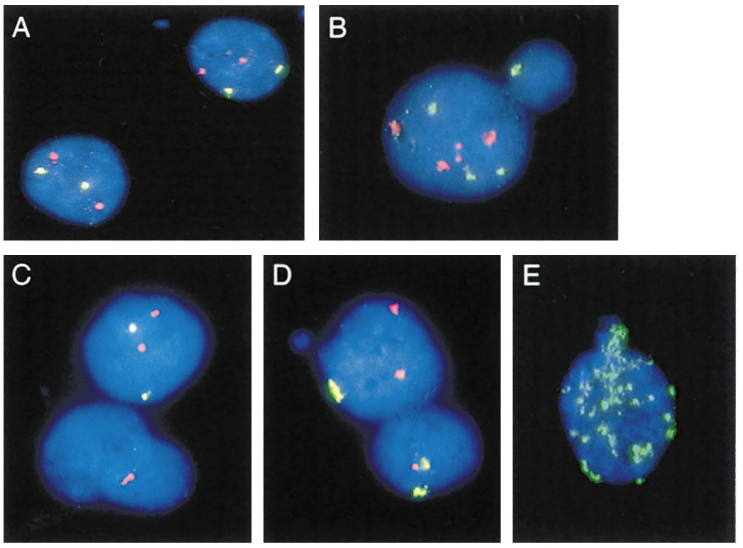

F

	chromosome analyzed	number of FISH signals per cell 0	1	2	3	4	≥5	% of cells off the mode
HCT116 (+/+)	7	0	2	98	0	0	0	2
	12	0	0	99	1	0	0	1
	17	0	2	96	2	0	0	4
	X	0	96	4	0	0	0	4
KO1 (-/-)	7	0	3	76	8	13	0	24
	12	0	7	70	7	14	2	30
	17	2	11	74	13	0	0	26
	X	14	68	15	2	1	0	32
KO2 (-/-)	7	1	15	69	8	5	2	31
	12	2	11	80	3	3	1	20
	17	2	7	83	4	3	1	17
	X	16	73	10	1	0	0	27

G

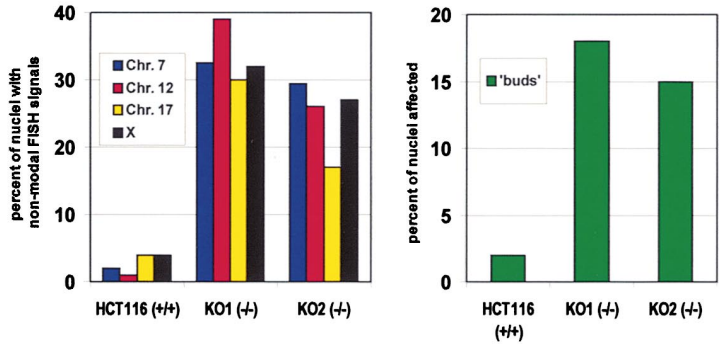

Figure 2. Chromosomal Instability in *hSecurin*$^{-/-}$ Cells

(A) *hSecurin*$^{+/+}$ (HCT116 parental) and *hSecurin*$^{-/-}$ cells (B–E) were subjected to FISH with centromeric probes specific for chromosome 7 (red) and chromosome 12 (green) (A–D), or with a pan-centromeric probe (E). Nuclear DNA was stained with DAPI (blue). (F) Chromosome gains and losses in *hSecurin*$^{+/+}$ and *hSecurin*$^{-/-}$ cells. The number of FISH signals per cell was determined for chromosomes 7, 12, 17, and X. The fraction of cells with FISH signals equal to the modal value of two (chromosomes 7, 12, and 17) or the modal value of one (X chromosome) is highlighted in yellow. Nonmodal cell populations accounting for 5% or more of the total are highlighted in green (for chromosome gains) and red (for chromosome losses). The total fraction of cells off the mode is given in the far-right column. (G) Left panel: graphical summary of the percentage of *hSecurin*$^{+/+}$ (HCT116) and *hSecurin*$^{-/-}$ (KO1, KO2) cells off the mode. Right panel: frequency of nuclear "bud" structures in *hSecurin*$^{+/+}$ and *hSecurin*$^{-/-}$ cells.

rial appeared to become stretched or deformed into two interconnected masses, giving rise to a "dumbbell"-type morphology (Figure 5B). The sharp separation between chromosomal masses that would indicate successful segregation of sister chromatids never appeared in these cells.

Despite their failure to execute anaphase, *hSecurin*$^{-/-}$ cells eventually exited mitosis, as the stretched chromatin masses decondensed to form the characteristic nuclear "buds" seen in fixed cells (Figure 5B, +70 min time point; compare with Figure 2B). Phase-contrast microscopy demonstrated that these anaphase-defective cells had exited mitosis without completing cytokinesis (data not shown).

Quantitative analysis of time lapse images was carried out to determine the relative timing of mitotic events in *hSecurin*$^{-/-}$ cells. The prophase-to-metaphase period (first sign of nuclear condensation to midline congression) and anaphase-to-telophase period (separation of chromosomes to nuclear decondensation) were similar in

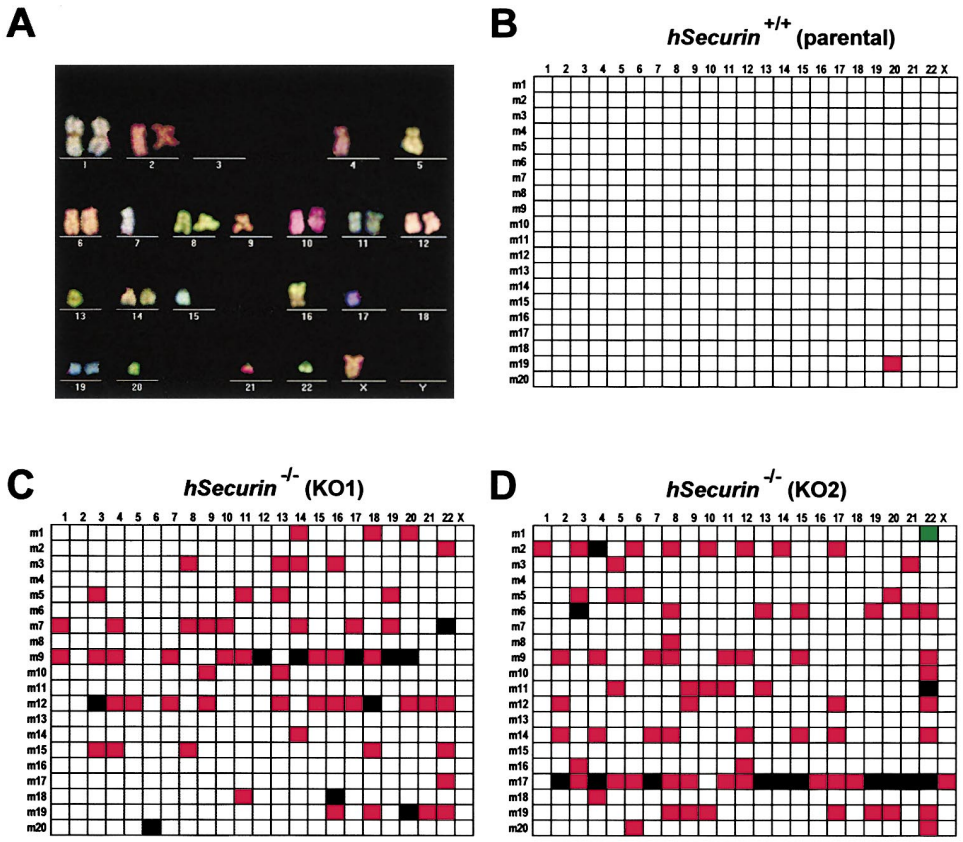

Figure 3. Multiplex-FISH Analysis of CIN Phenotype in *hSecurin*$^{-/-}$ Cells

(A) M-FISH karyotype from a *hSecurin*$^{-/-}$ cell metaphase.

(B–D) Graphical summary of M-FISH data from parental HCT116 cells (B) and *hSecurin*$^{-/-}$ cells (C and D). For each cell line, 20 metaphases (m1–m20) were painted by M-FISH and analyzed for alterations of chromosome structure and number. Loss of a single copy of a given chromosome is marked in red, loss of both copies is marked in black, and gain of a single copy is marked in green.

both *hSecurin*$^{+/+}$ and *hSecurin*$^{-/-}$ cells, though a small but statistically significant increase in the prophase-to-metaphase interval was observed in the hSecurin-deficient cells (19.8 $\pm$ 1.2 min versus 14.4 $\pm$ 0.7 min in the controls; Figure 5C). By contrast, the metaphase-to-anaphase interval was vastly increased in *hSecurin*$^{-/-}$ cells (48.4 $\pm$ 12.7 min versus 20.6 $\pm$ 1.5 min in the controls; Figure 5C). Thus, as assessed by both quantitative and qualitative criteria, anaphase execution was severely disrupted in human cells lacking securin.

Immunofluorescence experiments were next performed to examine the distribution of centromeres during mitosis. In these experiments, *hSecurin*$^{+/+}$ and *hSecurin*$^{-/-}$ cells in various stages of mitosis were stained with anti-centromere antibodies (ACA). The parental HCT116 cells exhibited patterns of centromere staining that typically characterize the individual stages of mitosis (Figures 6A–6D). In prophase, *hSecurin*$^{-/-}$ cells also showed the characteristic "double dot" pattern indicative of paired centromeres (Figures 6I). These paired centromeric signals then became tightly aligned, as would normally be expected during metaphase (Figure 6J). In anaphase, however, the centromeres of *hSecurin*$^{-/-}$ cells were aberrantly distributed, in striking contrast to control cells. Several paired centromeric dots remained at the metaphase plate, despite the fact that most of the sister chromatids had already separated, as seen by the migration of the bulk of centromeric signals away from the metaphase plate and toward the two spindle poles (Figures 6K and 6L).

To further demonstrate that chromosomes failed to properly segregate during anaphase, we carried out additional experiments using cyclin B as a marker for mitotic stage (Figures 6Q–6T). Anaphase cells were first identified by virtue of chromosome condensation and lack of cyclin B staining, then scored for unsegregated chromatids remaining at the metaphase plate. Strikingly, $\sim$30% of *hSecurin*$^{-/-}$ cells in anaphase (as assessed by the absence of cyclin B staining) still had paired sister chromatids left behind at the metaphase plate when most of the other chromosomes had segregated to the poles (Figures 6T and 6U).

Taken together, these results indicate that *hSecurin*$^{-/-}$ cells enter mitosis relatively normally, but then exhibit a major defect in the execution of anaphase associated with incomplete sister chromatid separation.

Regulation of Sister-Separating and Chromatid Cohesion Proteins by hSecurin

We next explored the consequences of securin deficiency on the separin protease. As recently reported, human separin exists as several cell cycle regulated

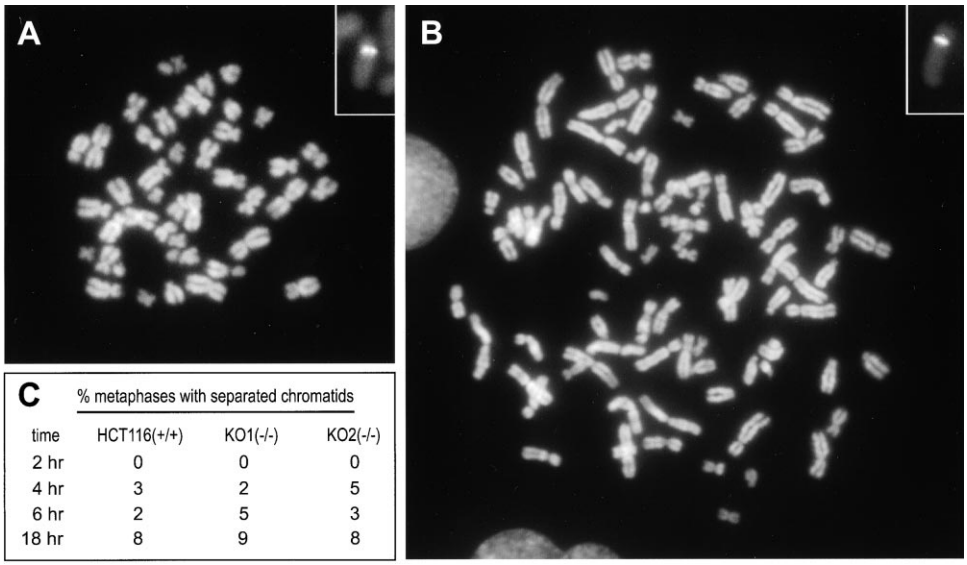

C

% metaphases with separated chromatids			
time	HCT116(+/+)	KO1(-/-)	KO2(-/-)
2 hr	0	0	0
4 hr	3	2	5
6 hr	2	5	3
18 hr	8	9	8

Figure 4. Sister Chromatid Cohesion Is Maintained in *hSecurin*$^{-/-}$ Cells after Spindle Damage

Metaphase spreads were prepared from *hSecurin*$^{+/+}$ cells (A) and *hSecurin*$^{-/-}$ cells (B) after a 4 hr treatment with colcemid. Chromosomes were either stained directly with DAPI (A and B) or hybridized with a FISH probe specific for the centromeric region of chromosome 12 (inset panels in [A] and [B]). Note that the aneuploid karyotype in (B) lacks any detectable sister chromatid separation, and that the FISH signals remain tightly coupled. (C) Quantitation of sister chromatid separation in metaphase spreads. Parental HCT116 cells and two independent *hSecurin*$^{-/-}$ cell lines were treated with colcemid for up to 18 hr. Individual metaphase spreads (n = 200) were scored for the presence of one or more pairs of separated sister chromatids.

forms (Waizenegger et al., 2000). During mitosis, separin undergoes proteolytic cleavage to produce carboxy-terminal fragments containing the core "separase domain" that is conserved among all separin proteins (Waizenegger et al., 2000; Figure 7A, left panel). Intriguingly, the mitotic-specific p60 separin cleavage product was dramatically reduced in log phase *hSecurin*$^{-/-}$ cells (Figure 7A, right panel).

To confirm these results, separin cleavage was analyzed in cells synchronized by sequential thymidine-aphidicolin treatments. The synchronization and cell cycle progression were equivalent in *hSecurin*$^{+/+}$ and *hSecurin*$^{-/-}$ cells, as judged by FACS analysis (Figure 7B) and by fluctuation in cyclin B and phosphorylated histone H3 (Figure 7C). In control cells, the mitotic-specific separin p60 accumulated as cells progressed through mitosis, while the abundance of full-length separin declined (Figure 7C, left panel; 12–24 hr time points). In synchronized *hSecurin*$^{-/-}$ cells, full-length separin p200 was also present, albeit at lower levels (Figure 7C, right panel). As in control cells, the abundance of separin p200 declined as cells completed mitosis. However, the mitotic-specific p60 form of separin could not be detected in *hSecurin*$^{-/-}$ cells, in contrast to the parental cells (Figure 7C, right panel). The absence of detectable p60 cleavage product and the reduction in full-length separin p200 suggest that the cleavage and/or stability of separin is reduced in *hSecurin*$^{-/-}$ cells.

We next examined the biochemical properties of the separin protease in vitro, as assayed by its ability to cleave the human cohesin subunit Scc1. While the vast majority of Scc1 dissociates from chromosomes prior to metaphase in vertebrate cells (Losada et al., 1998; Sumara et al., 2000), a small fraction remains bound to centromeric regions and appears to undergo site-specific cleavage at the onset of anaphase (Waizenegger et al., 2000). This cleavage reaction has been reconstituted in vitro using immunoprecipitated separin complexes that are first incubated with *Xenopus* extracts as a source of mitotic APC, and then assayed for cleavage of Scc1 into two distinct fragments of 55 kDa and 115 kDa (Waizenegger et al., 2000).

In the presence of mitotic *Xenopus* extracts, a large fraction of full-length separin p200 from *hSecurin*$^{+/+}$ cells was proteolytically cleaved, as shown by the increased intensity of the cleavage products and a decrease in the full-length p200 form (Figure 8A, top panel, lanes 1 and 2). This reaction also triggered degradation of hSecurin (Figure 8A, bottom panel).

The amount of separin protein in extracts containing equal amounts of protein was significantly reduced in mitotically synchronized *hSecurin*$^{-/-}$ cells (Figure 8A, lane 3), consistent with the immunoblotting results shown in Figure 7. The level of full-length separin p200 did not change after incubation with *Xenopus* extracts. Moreover, the separin complexes from *hSecurin*$^{-/-}$ cells exhibited no cleavage activity of the Scc1 substrate, even after a 60 min incubation period (Figure 8B, compare lanes 1–6 with lanes 17–21).

We also tested excess amounts of *hSecurin*$^{-/-}$ cell extract in our in vitro assay. These titration experiments permitted us to examine the role of hSecurin in the specific activity of separin protease. The amount of p200 separin was found to be ~4-fold lower in *hSecurin*$^{-/-}$ cells than in control cells (compare lane 5 with lane 1 in Figure 8A). Little proteolytic processing of separin was observed in these extracts, even when equal amounts of the p200 separin were added (Figure 8A; compare lanes

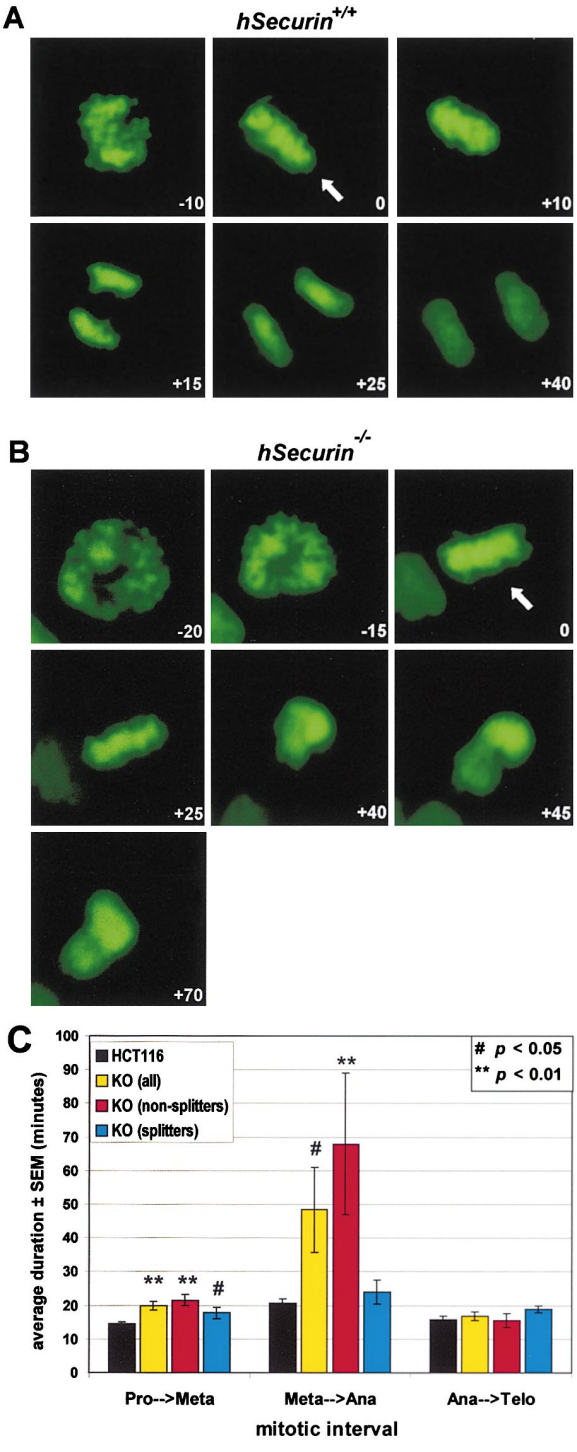

Figure 5. Defective Execution of Anaphase in *hSecurin*$^{-/-}$ Cells

Mitotic *hSecurin*$^{+/+}$ cells (A) and *hSecurin*$^{-/-}$ cells (B) stably expressing a histone H2B-GFP fusion protein were subjected to time lapse fluorescence microscopy. Arrows in (A) and (B) point to aligned metaphase chromosomes; this mitotic event was defined as time 0. Negative and positive values in the bottom right corner of individual frames indicate times (in minutes) before or after metaphase alignment. (C) Quantitative analysis of mitotic intervals in *hSecurin*$^{+/+}$ and *hSecurin*$^{-/-}$ cells. Eighteen cells of each genotype were followed by time lapse microscopy, and the duration of the indicated mitotic intervals was determined as described in Experimental Procedures. For statistical analyses, *hSecurin*$^{-/-}$ cells were either treated as a single group (yellow bars), or divided into two distinct subgroups based on whether they eventually completed chromosome segregation ("splitters," blue bars) or not ("non-splitters," red bars). All data were evaluated by two-tailed Student's t test. # and ** symbols mark statistically significant (#, $p < 0.05$; **, $p < 0.01$) deviations from the wild-type pattern. SEM, standard error of measurement.

5–8 with lanes 1 and 2). Moreover, under these conditions, the separin protease from *hSecurin*$^{-/-}$ cells was less potent in cleaving the Scc1 substrate than that isolated from control cells (Figure 8B; compare lanes 7–11 with lanes 17–21).

In summary, our biochemical data revealed at least three distinct effects of hSecurin deletion on the separin protease. First, mitotically synchronized *hSecurin*$^{-/-}$ cells have reduced levels of separin protein. Second, the mitosis-specific processing of the separin protease to the p60 form was impaired in the absence of hSecurin. Third, separin protease that had no opportunity to interact with hSecurin had reduced specific activity on its substrate, Scc1.

To begin to address the physiological relevance of these in vitro observations, we examined whether hSecurin deficiency affected Scc1 cleavage in vivo. *hSecurin*$^{+/+}$ and *hSecurin*$^{-/-}$ cells were transfected with a myc epitope-tagged Scc1 expression vector (Waizenegger et al., 2000) and synchronized in a metaphase-like state with nocodazole. Following release from the nocodazole block, samples were collected at various time points, and the cleavage of Scc1-myc protein was assayed by immunoblotting. In *hSecurin*$^{+/+}$ cells, a ~55 kDa cleavage product of Scc1 appeared ~2 hr after release (Figure 8C). This time point corresponds to the onset of cyclin B degradation, a biochemical indicator of anaphase (Figure 8C). By contrast, a much lower level of the 55 kDa cleavage product was observed in *hSecurin*$^{-/-}$ cells, even though cells continued to degrade cyclin B and exit mitosis (Figure 8C and data not shown).

Discussion

Mutations in the yeast *PDS1* gene uncouple anaphase from the mitotic spindle checkpoint, allowing sister chromatid separation in cells treated with microtubule inhibitors (Yamamoto et al., 1996a; Ciosk et al., 1998). We performed similar experiments on *hSecurin*$^{-/-}$ cells with the expectation that such cells would separate their sister chromatids in the presence of spindle poisons. However, we found no evidence for chromatid separation in *hSecurin*$^{-/-}$ cells even after prolonged incubation in nocodazole or colcemid (Figure 4). Thus, it appears that the mitotic spindle checkpoint can inhibit sister chromatid separation in the absence of securin in mammalian cells, unlike the situation in budding yeast.

In contrast, the deletion of *hSecurin* appeared to inhibit the faithful execution of anaphase. This phenotype was similar to that observed in fission yeast and *Drosophila* with mutations in *hSecurin* homologs (see Introduction) and in human cells expressing noncleavable Scc1, which also appear to block in anaphase (S. Hauf, I.C.W., and J.-M.P., unpublished data). Time lapse experiments and immunofluorescence microscopy showed

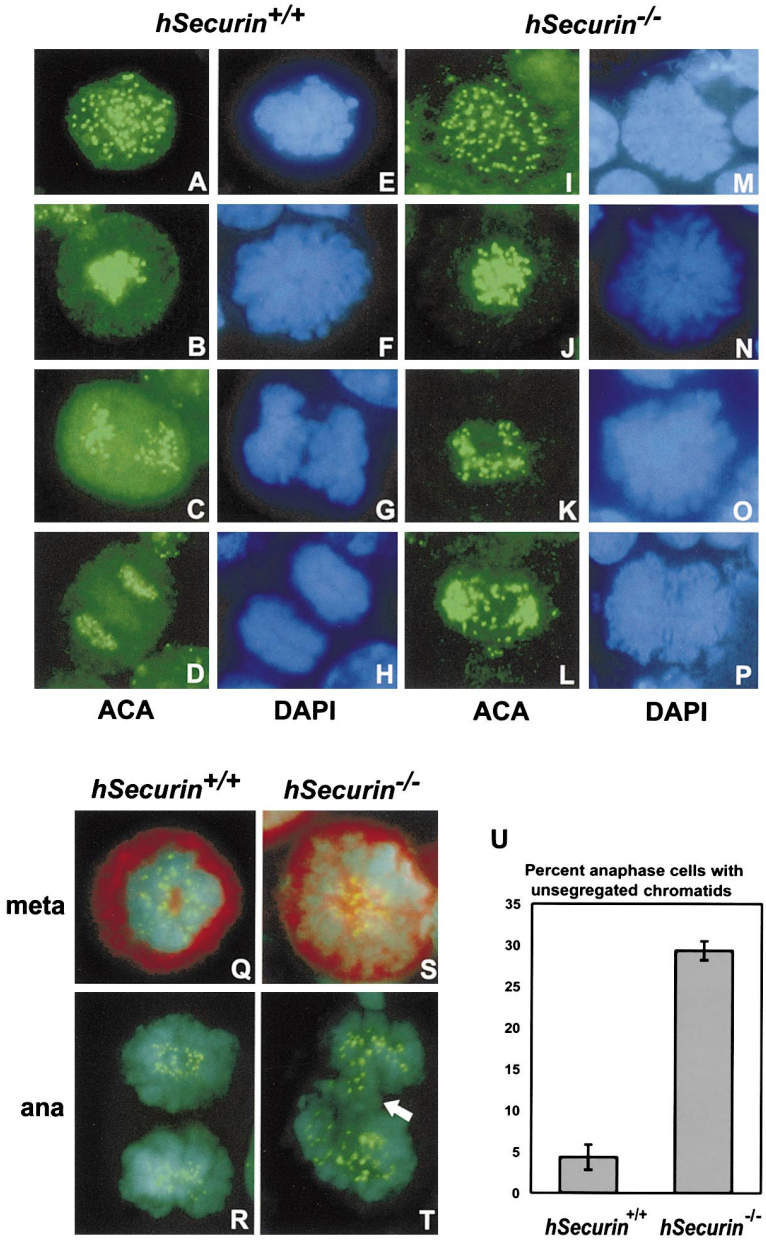

Figure 6. Defective Sister Chromatid Separation in *hSecurin*$^{-/-}$ Cells

Mitotic *hSecurin*$^{+/+}$ cells (A–H) and *hSecurin*$^{-/-}$ cells (I–P) were stained with anti-centromere antibodies (ACA; A–D and I–L). Nuclear DNA was counterstained with DAPI (E–H and M–P). First row: prophase cells, showing the characteristic "double-dot" pattern of paired centromeres. Second row: metaphase cells, with centromeres tightly aligned on the spindle (axis perpendicular to plane of the figure). Third and fourth rows: anaphase and telophase cells. Note that centromeric signals in *hSecurin*$^{+/+}$ cells showed complete separation of sister chromatids and migration of centromeres to both poles (C and D), whereas some centromeres in *hSecurin*$^{-/-}$ cells failed to segregate and remained associated with the metaphase plate (K and L).

(Q–U) Quantitation of chromatid separation defect in anaphase *hSecurin*$^{-/-}$ cells. Mitotic *hSecurin*$^{+/+}$ cells (Q and R) and *hSecurin*$^{-/-}$ cells (S and T) were double-stained with ACA (green) and anti-cyclin B antibodies (red). Metaphase cells stained strongly for cyclin B (Q and S), while anaphase cells showed little or no cyclin B staining (R and T). Arrow in (T) marks unsegregated sister chromatids trapped at the metaphase plate. (U) Percentage of anaphase cells with unsegregated sister chromatids at the metaphase plate was determined from 150 cells of each genotype (50 cells each in three separate experiments).

that hSecurin-deficient human cells carried out futile attempts at chromatid separation, resulting in an abnormal anaphase process (Figures 5 and 6). The final outcome of this process was cells with budded nuclei (Figure 2G), chromosomal instability (Figure 2F), and gross aneuploidy (Figure 3).

We propose a two-step "trigger lock" model that is consistent with our biochemical and genetic analyses and with published data on securin mutants in other organisms (Nasmyth et al., 2000; Yanagida, 2000). According to this model, full-length separin p200 would bind its inhibitor (securin) to "cock the trigger" for anaphase. APC activation would then "pull the trigger" by degrading securin, allowing separin protease to be activated, cohesins to be cleaved, and chromatid segregation to occur. According to this model, separin that has never been bound to securin would be largely inactive—a safety lock on the trigger mechanism.

Under this model, securin could "cock" the separin protease by at least two distinct mechanisms. First, securin probably stabilizes the separin enzyme complex prior to anaphase. This was suggested by the reduced levels of full-length separin p200 in synchronized cells lacking hSecurin. However, this cannot be the sole mechanism of separin regulation, as logarithmically growing *hSecurin*$^{+/+}$ and *hSecurin*$^{-/-}$ cells, unperturbed by synchronization, have comparable levels of full-length p200 separin but very different levels of the p60 cleavage product (Figure 7A). This observation, together with our in vitro data (Figure 8A), indicate that *hSecurin*$^{-/-}$ cells have an additional defect in the APC-dependent cleavage of full-length separin.

It is not yet clear which form of separin protease is the active form of the enzyme. Therefore, we cannot determine whether the lack of separin cleavage in *hSecurin*$^{-/-}$ cells is directly responsible for the reduction

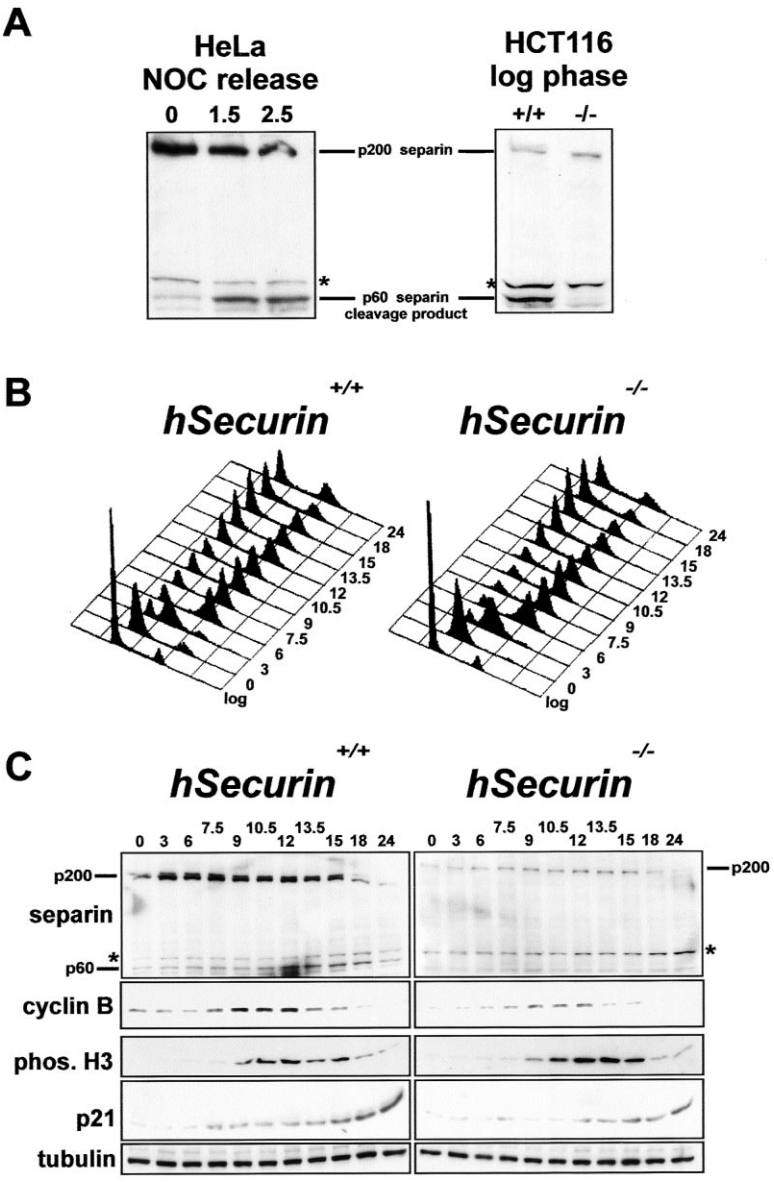

Figure 7. Separin Regulation Is Defective in *hSecurin*$^{-/-}$ Cells

(A) Lysates from HeLa cells arrested with nocodazole and released for 1.5 or 2.5 hr (left panel) and from log phase *hSecurin*$^{+/+}$ and *hSecurin*$^{-/-}$ cells (right panel) were probed with antibodies to separin. The positions of the full-length (p200) and cleaved (p60) forms of separin are indicated. Asterisks (*) mark a nonspecific background band.

(B) Cell cycle analysis of separin dynamics. *hSecurin*$^{+/+}$ cells (left panel) and *hSecurin*$^{-/-}$ cells (right panel) were synchronized by sequential thymidine-aphidicolin blocks, and flow cytometry was performed as described in Experimental Procedures. Numbers indicate hours after release from the aphidicolin block.

(C) Lysates from synchronized cells in (B) were analyzed by immunoblotting with antibodies to separin. Blots were also probed with antibodies to phosphorylated histone H3, cyclin B, and the CDK inhibitor p21$^{WAF1/CIP1}$ as markers of mitotic entry and exit. The positions of the full-length (p200) and cleaved p60 forms of separin are indicated. Asterisks (*) indicate a nonspecific band. α-Tubulin was used as a loading control.

in separin protease activity. Many proteases are synthesized as large inactive polypeptides that become activated only after specific proteolytic cleavages under highly regulated conditions (e.g., zymogens and caspases; Stennicke and Salvesen, 2000). In support of this analogy is the recent finding that separins actually belong to the same family of cysteine proteases as the caspases (Uhlmann et al., 2000). However, it is equally possible that separin cleavage is simply a consequence of separin activation. In this case, the failure to cleave p200 separin in the absence of hSecurin would be a direct reflection of reduced separin protease activity, not the cause of it. Further work in defining the active forms of the separin protease and in characterizing uncleavable forms of separin will be essential in clarifying the exact biochemical events leading to sister chromatid separation.

One strength of the morphologic observations reported in this study is that they were made on cells normally traversing mitosis in the absence of microtubule inhibitors or cell cycle blockers. It is important to note that anaphase eventually did occur in most of the *hSecurin*$^{-/-}$ cells under these circumstances. Whether this resulted from residual separin protease activity in vivo, from cleavage of cohesins by other proteins, or from cohesin dissociation from chromatids in the absence of cleavage could not be determined from our experiments. Interestingly, we could detect some Scc1 cleavage in vitro using an excess of *hSecurin*$^{-/-}$ cell extracts (Figure 8B), and a very low level of Scc1 cleavage in vivo was consistently observed in anaphase *hSecurin*$^{-/-}$ cells (Figure 8C). These data suggest that a basal level of separin protease activity persists in hSecurin-deficient cells, which may explain why they remain viable.

Finally, our results show that disruption of a single component of the complex of proteins responsible for sister chromatid cohesion (securin, separin, cohesins,

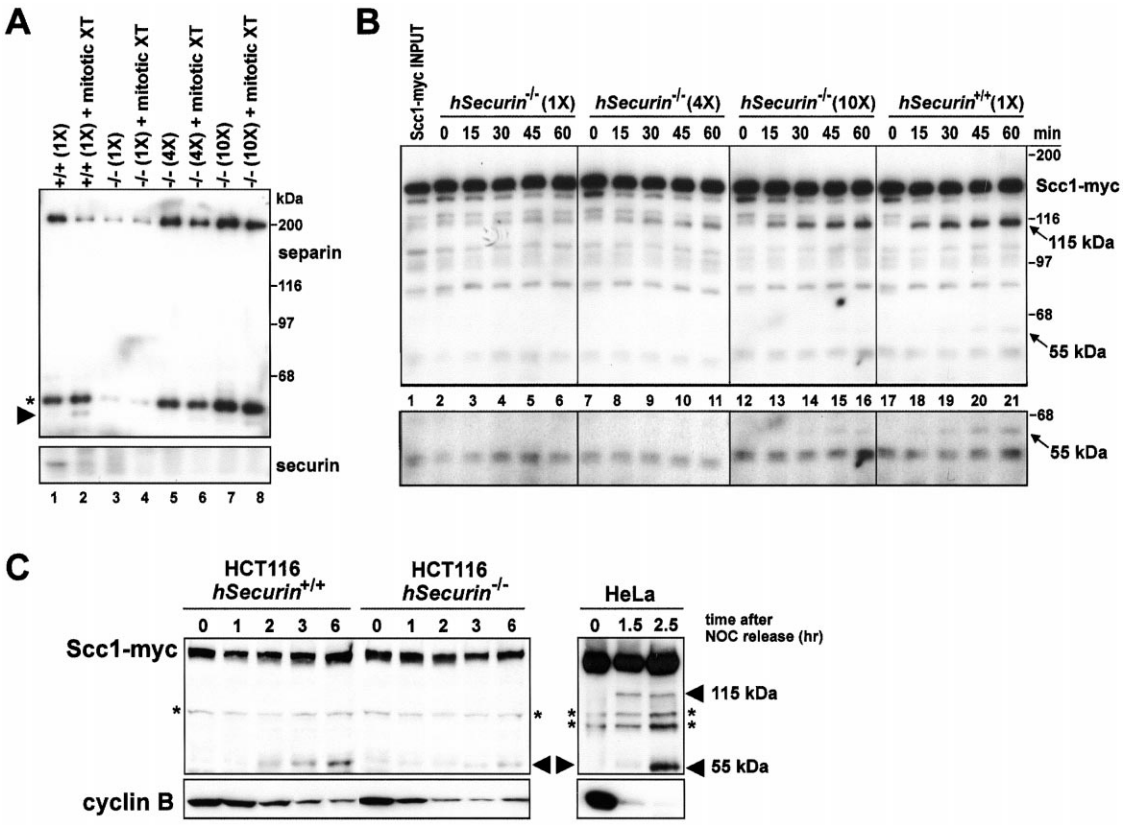

Figure 8. Securin Is Necessary for APC-Dependent Proteolytic Processing and Activation of Separin Protease In Vitro

(A) Separin was immunoprecipitated from nocodazole-arrested *hSecurin*$^{+/+}$ and *hSecurin*$^{-/-}$ cells. To vary the amounts of separin, different amounts of *hSecurin*$^{-/-}$ cell extract were used for immunoprecipitation, where (1X) denotes the amount of control cell extract (2 mg protein) that was used in the assay. Immobilized complexes were analyzed by immunoblotting before and after incubation in mitotic *Xenopus* extracts (+ mitotic XT). Processing of p200 separin to faster migrating fragments (asterisk and arrowhead, top panel) and degradation of securin (bottom panel) were assessed by immunoblotting with appropriate antibodies.

(B) Separin immunoprecipitates isolated and activated as in (A) were incubated with in vitro translated human Scc1-myc as a substrate (Scc1-myc INPUT). At the indicated time points, aliquots of the reaction were withdrawn for analysis. Arrows indicate the 115 and 55 kDa Scc1-myc cleavage products. High-contrast image of the bottom portion of the same blot confirmed the lack of detectable 55 kDa Scc1-myc cleavage product in lanes 1–13.

(C) *hSecurin*$^{+/+}$ and *hSecurin*$^{-/-}$ HCT116 cells were transfected with a Scc1-myc expression construct and synchronized in mid-mitosis with nocodazole. Cells were released from the nocodazole block and collected at various time points. Nocodazole-synchronized HeLa cells expressing Scc1-myc were used as a positive control. Lysates were analyzed by immunoblotting with myc antibody (top panels) and cyclin B antibody (bottom panels). Arrowheads mark the position of the 115 and 55 kDa Scc1-myc cleavage products. The 115 kDa band was readily detected in HeLa cells but not in HCT116 cells, suggesting preferential utilization of the carboxy-terminal cleavage site in HCT116 in vivo. Asterisks (*) indicate Scc1-myc fragments present throughout the cell cycle.

Cdc20, APC components) can convert karyotypically stable euploid cells to unstable aneuploid ones. This instability involved losses of whole chromosomes in the absence of the chromosome breaks and abnormal DNA repair processes that have also been invoked as potential causes of CIN. Genetic alterations resulting in inactivation of *hSecurin* have not been observed in human cancers, though this gene has been reported to be expressed at abnormally high levels in some cancers (Dominguez et al., 1998; Saez et al., 1999; Heaney et al., 2000). Our results show that it is not difficult to genetically convert a chromosomally stable cancer cell into an unstable one that retains the capacity to proliferate robustly. A search for naturally occurring inactivating mutations in the genes that control chromatid cohesion and segregation may therefore provide further clues to the nature of CIN in human cancers.

Experimental Procedures

Inactivation of the *hSecurin* Locus by Homologous Recombination

Methods for generation of somatic cell knockouts in HCT116 have been described (Waldman et al., 1996; Bunz et al., 1998; Chan et al., 1999; Rhee et al., 2000) and were modified to generate *hSecurin*$^{-/-}$ cell lines. In brief, primers PTTG1-F1 and PTTG1-R3 were used to screen a human BAC library (Research Genetics) for genomic clones spanning the *hSecurin/hPTTG1* locus. Elongase (Life Technologies) was used to amplify a 1.3 kb 5′ targeting element (using primers PTTG1-Lforward and PTTG1-L1.3reverse) and a ~5 kb 3′ targeting element (using primers PTTG1-Rforward and PTTG1-Rreverse). The resulting PCR products were cloned into the targeting vectors pFredA and pFredB, respectively, to create plasmids pFredA-PTTG1-L1.3 and pFredB-PTTG-R5. This new "two-vector" targeting system was developed in an effort to reduce the background rate of Geneticin-resistant colonies arising from nonhomologous integration events (F.B., B.V., K.K., unpublished data). These constructs were digested with KpnI and SalI, respectively, and co-

transfected into HCT116 cells using the Lipofectamine reagent (Life Technologies). Stably transfected cells were selected in McCoy's 5A medium supplemented with 10% fetal bovine serum (FBS) and 0.4 mg/ml Geneticin. Genomic DNA was isolated from pools of Geneticin-resistant clones (~10 clones/pool) and screened by PCR using primers PTTG1-A1 and NEOreverse. Individual clones were obtained by limiting dilution of positive pools and rescreened by PCR. Candidate *hSecurin*$^{+/-}$ clones were confirmed by additional PCR analyses and by loss of a G/A polymorphism at nucleotide 1662 of the published genomic sequence (data not shown). Excision of the integrated *loxP-NEO-loxP* cassette was effected by transfection with a Cre recombinase expression plasmid (pΔE1-creHA) and isolation of individual Geneticin-sensitive clones. The remaining wild-type allele was inactivated by repeating the targeting procedure described above. Finally, four additional PCR primers (PTTG-F6, PTTG-R1; PTTG-gen01, PTTG-R4) were used to define two STS markers spanning the first intron and second exon of the *hSecurin* locus that were homozygously deleted in *hSecurin*$^{-/-}$ cells. For Southern blotting, genomic DNAs were digested with MseI, transferred to Zeta Probe membrane (Bio-Rad), and hybridized with a [^{32}P]-labeled probe corresponding to the 5′ *hSecurin* targeting element. Additional details, including sequences of all PCR primers used in this study, are available from the authors upon request.

Fluorescence In Situ Hybridization (FISH) Analysis of Chromosome Loss

Methods for FISH analysis with chromosome-specific centromeric probes and quantitative analysis of chromosome loss rates have been described (Lengauer et al., 1997). A pan-centromeric FISH probe (IDbright Pan-Centromeric) was obtained from ID Labs Inc. and used according to the manufacturer's directions. To prepare metaphase spreads, cells were treated with 0.1 μg/ml colcemid (KaryoMax, Life Technologies) for the indicated time periods and processed by standard methods. Multiplex-FISH analysis was performed exactly as described (Speicher et al., 1996). The full karyotype of HCT116 cells was confirmed as 45,X,-Y, der(10)dup(10)(q24q26)t(10;16)(q26;q24), der(16)t(8;16)(q13;p13), der(18)t(17;18)(q21;p11.3).

Time Lapse Imaging of Mitosis in Live Cells

HCT116 and *hSecurin*$^{-/-}$ cells stably transfected with pBOS-histone H2B-GFP (Kanda et al., 1998) were analyzed on a Nikon TE200 inverted microscope with 40× objective enclosed in a temperature-controlled incubator. Images were acquired with a Princeton CCD camera at intervals ranging from 1 to 10 min and analyzed using the MetaMorph software program (Universal Imaging). For quantitation of mitotic intervals, the prophase-to-metaphase period was defined as the time elapsed from the first sign of nuclear condensation to midline alignment of chromosomes. The metaphase-to-anaphase period was defined as the interval from alignment to partial or total separation of chromatin into two masses, and the anaphase-to-telophase period was defined as the time from chromosome separation to nuclear decondensation.

Immunofluorescence Microscopy of Centromeres during Mitosis

Mitotic cells were obtained by gently tapping flasks of logarithmically growing *hSecurin*$^{+/+}$ and *hSecurin*$^{-/-}$ cells. Cells were washed with PBS and fixed for 10 min in 4% paraformaldehyde (in PBS). Aliquots of the cell suspension were cytocentrifuged onto glass slides and permeabilized in PBS + 0.1% Triton X-100 for 5 min. Slides were incubated in blocking solution (10% fetal bovine serum in PBS) for 30 min. Human anti-centromere antibodies (ACA) were obtained from Sigma (ANA-C) and used at a dilution of 1:25 in blocking solution for 60 min. Where indicated, anti-cyclin B monoclonal antibody (Santa Cruz) was used at a 1:200 dilution. Slides were then washed three times in PBS + 0.05% Tween-20 and incubated with Alexa 488-conjugated anti-human and Alexa 594-conjugated anti-mouse secondary antibodies (Molecular Probes) at 1:100 for 60 min. Slides were washed as above, counterstained with DAPI, and mounted in antifade solution prior to fluorescence microscopy.

Cell Cycle Synchronization, FACS Analysis, and Immunoblotting

Cells were synchronized at the G1/S phase transition by sequential thymidine and aphidicolin blocks. Briefly, cells were cultured in McCoy's 5A medium plus 10% FBS supplemented with 2.5 mM thymidine for 18 hr, then washed twice with Hank's balanced salt solution (HBSS), and incubated in McCoy's medium plus 10% FBS. After 8 hr, aphidicolin was added to a final concentration of 2 μg/ml. After 15 hr, cells were washed twice with HBSS and incubated in fresh McCoy's medium + 10% FBS. At various time points, cells were harvested and washed with ice-cold phosphate-buffered saline. A portion of harvested cells was fixed and stained in formaldehyde/Hoechst 33258 solution (Bunz et al., 1998), and the remaining cells were frozen at −80°C. FACS analysis was performed on a LSR Flow Cytometer (Becton Dickinson) using the CellQuest software package.

Protein extracts were prepared by lysing cells on ice in HB2 buffer (50 mM HEPES, [pH 7.5], 0.5% NP-40, 10% glycerol, 100 mM NaCl, 10 mM Na pyrophosphate, 5 mM β-glycerophosphate, 50 mM NaF, 0.3 mM Na_3VO_4, 1 mM DTT, 1 mM PMSF, and 1× complete protease inhibitor cocktail [Roche]), followed by brief sonication and centrifugation at 10,000 × *g* for 15 min at 4°C. Immunoblotting was performed on Immobilon P membranes (MilliPore) according to the manufacturer's instructions. Antibodies to hSecurin were generated by immunizing rabbits with peptides VDKENGEPGTRVVAKDGLC and LDEERELEKLFQLGC, followed by affinity purification on a peptide matrix (QCB/BioSource). Antibodies to human Scc1 and separin have been described (Waizenegger et al., 2000). Commercially available antibodies to cyclin B (Santa Cruz), phosphorylated histone H3 (Upstate Biotechnology), p21$^{WAF1/CIP1}$, and α-tubulin (Oncogene Science) were used as recommended by the manufacturers. Signals were developed using the Renaissance Plus Enhanced Chemiluminescence Reagent (New England Nuclear).

Scc1 In Vitro Cleavage Assays

In vitro cleavage of Scc1 by separin was performed as described (Waizenegger et al., 2000) with the following modifications: separin was immunoprecipitated from extracts of nocodazole-arrested HCT116 cells (*hSecurin*$^{+/+}$) containing 2 mg total protein, or from extracts of nocodazole-arrested *hSecurin*$^{-/-}$ cells containing 2, 8, or 20 mg of total protein. Recombinant human Scc1-myc substrate was synthesized by coupled in vitro transcription-translation reactions (Promega) and used as a separin protease substrate. Scc1 cleavage assays contained 23 ng/μl recombinant human Polo-like kinase 1 (kindly provided by I. Sumara, IMP, Vienna, Austria). Aliquots of the reaction mixture were withdrawn at various times and added to SDS-PAGE sample buffer for analysis of Scc1 cleavage by immunoblotting.

Scc1 Cleavage In Vivo

An expression plasmid encoding human Scc1 tagged at the carboxyl terminus with nine copies of the myc epitope (pcDNA-hScc1-myc) was transfected into HCT116 *hSecurin*$^{+/+}$ and *hSecurin*$^{-/-}$ cells. Approximately 24 hr after transfection, 0.2 μg/ml nocodazole was added to arrest cells in a metaphase-like state. After 15 to 18 hr, cells were washed three times with HBSS and returned to nocodazole-free medium. Cells were harvested at the indicated time points. HeLa cells expressing Scc1-myc (Waizenegger et al., 2000) were used as a positive control. Preparation of cell lysates and detection of Scc1-myc cleavage products by immunoblotting were performed as described above.

Acknowledgments

We would like to thank Leslie Meszler from the Cell Imaging Core Facility for excellent technical assistance. This work was supported by the Clayton Fund, the Concern Foundation, and NIH grants CA 43460, CA 57345, CA 62924, GM 41690, and GM07309. Research in the lab of J.-M.P. is supported by Boehringer Ingelheim and by grants from the Austrian Science Fund and the Austrian Research Promotion Fund. Research in the lab of M.R.S. is supported by the Deutsche Krebshilfe. Under an agreement between CalBiochem and Johns Hopkins University, K.W.K. and B.V. are entitled to a share of the sales royalty for the anti-p21 antibodies received by the University from CalBiochem. The terms of this arrangement are being managed by the University in accordance with its conflict of interest

policies. P.V.J. is a fellow of the Damon Runyon-Walter Winchell Foundation's Cancer Research Fund.

Received November 17, 2000; April 19, 2001.

References

Amon, A. (1999). The spindle checkpoint. Curr. Opin. Genet. Dev. *9*, 69–75.

Bunz, F., Dutriaux, A., Lengauer, C., Waldman, T., Zhou, S., Brown, J.P., Sedivy, J.M., Kinzler, K.W., and Vogelstein, B. (1998). Requirement for p53 and p21 to sustain G2 arrest after DNA damage. Science *282*, 1497–1501.

Cahill, D.P., Lengauer, C., Yu, J., Riggins, G.J., Willson, J.K., Markowitz, S.D., Kinzler, K.W., and Vogelstein, B. (1998). Mutations of mitotic checkpoint genes in human cancers. Nature *392*, 300–303.

Cahill, D.P., Kinzler, K.W., Vogelstein, B., and Lengauer, C. (1999). Genetic instability and Darwinian selection in tumours. Trends Cell Biol. *9*, M57–M60.

Chan, T.A., Hermeking, H., Lengauer, C., Kinzler, K.W., and Vogelstein, B. (1999). 14–3-3σ is required to prevent mitotic catastrophe after DNA damage. Nature *401*, 616–620.

Chen, R.H., Waters, J.C., Salmon, E.D., and Murray, A.W. (1996). Association of spindle assembly checkpoint component XMAD2 with unattached kinetochores. Science *274*, 242–246.

Ciosk, R., Zachariae, W., Michaelis, C., Shevchenko, A., Mann, M., and Nasmyth, K. (1998). An ESP1/PDS1 complex regulates loss of sister chromatid cohesion at the metaphase to anaphase transition in yeast. Cell *93*, 1067–1076.

Cohen-Fix, O., Peters, J.M., Kirschner, M.W., and Koshland, D. (1996). Anaphase initiation in Saccharomyces cerevisiae is controlled by the APC-dependent degradation of the anaphase inhibitor Pds1p. Genes Dev. *10*, 3081–3093.

Dobles, M., Liberal, V., Scott, M.L., Benezra, R., and Sorger, P.K. (2000). Chromosome missegregation and apoptosis in mice lacking the mitotic checkpoint protein Mad2. Cell *101*, 635–645.

Dominguez, A., Ramos-Morales, F., Romero, F., Rios, R.M., Dreyfus, F., Tortolero, M., and Pintor-Toro, J.A. (1998). hpttg, a human homologue of rat pttg, is overexpressed in hematopoietic neoplasms. Evidence for a transcriptional activation function of hPTTG. Oncogene *17*, 2187–2193.

Duesberg, P., Rasnick, D., Li, R., Winters, L., Rausch, C., and Hehlmann, R. (1999). How aneuploidy may cause cancer and genetic instability. Anticancer Res. *19*, 4887–4906.

Fang, G., Yu, H., and Kirschner, M.W. (1998). The checkpoint protein MAD2 and the mitotic regulator CDC20 form a ternary complex with the anaphase-promoting complex to control anaphase initiation. Genes Dev. *12*, 1871–1883.

Funabiki, H., Kumada, K., and Yanagida, M. (1996a). Fission yeast Cut1 and Cut2 are essential for sister chromatid separation, concentrate along the metaphase spindle and form large complexes. EMBO J. *15*, 6617–6628.

Funabiki, H., Yamano, H., Kumada, K., Nagao, K., Hunt, T., and Yanagida, M. (1996b). Cut2 proteolysis required for sister-chromatid separation in fission yeast. Nature *381*, 438–441.

Gardner, R.D., and Burke, D.J. (2000). The spindle checkpoint: two transitions, two pathways. Trends Cell Biol. *10*, 154–158.

Gemma, A., Seike, M., Seike, Y., Uematsu, K., Hibino, S., Kurimoto, F., Yoshimura, A., Shibuya, M., Harris, C.C., and Kudoh, S. (2000). Somatic mutation of the hBUB1 mitotic checkpoint gene in primary lung cancer. Genes Chromosomes Cancer *29*, 213–218.

Glotzer, M. (1999). Chromosome segregation: Samurai separation of Siamese sisters. Curr. Biol. *9*, R531–R534.

Heaney, A.P., Singson, R., McCabe, C.J., Nelson, V., Nakashima, M., and Melmed, S. (2000). Expression of pituitary-tumour transforming gene in colorectal tumours. Lancet *355*, 716–719.

Imai, Y., Shiratori, Y., Kato, N., Inoue, T., and Omata, M. (1999). Mutational inactivation of mitotic checkpoint genes, hsMAD2 and hBUB1, is rare in sporadic digestive tract cancers. Jpn. J. Cancer Res. *90*, 837–840.

Kalitsis, P., Earle, E., Fowler, K.J., and Choo, K.H. (2000). Bub3 gene disruption in mice reveals essential mitotic spindle checkpoint function during early embryogenesis. Genes Dev. *14*, 2277–2282.

Kanda, T., Sullivan, K.F., and Wahl, G.M. (1998). Histone-GFP fusion protein enables sensitive analysis of chromosome dynamics in living mammalian cells. Curr. Biol. *8*, 377–385.

King, R.W., Deshaies, R.J., Peters, J.M., and Kirschner, M.W. (1996). How proteolysis drives the cell cycle. Science *274*, 1652–1659.

Kinzler, K.W., and Vogelstein, B. (1996). Lessons from hereditary colon cancer. Cell *87*, 159–170.

Lee, H., Trainer, A.H., Friedman, L.S., Thistlethwaite, F.C., Evans, M.J., Ponder, B.A., and Venkitaraman, A.R. (1999). Mitotic checkpoint inactivation fosters transformation in cells lacking the breast cancer susceptibility gene, Brca2. Mol. Cell *4*, 1–10.

Leismann, O., Herzig, A., Heidmann, S., and Lehner, C.F. (2000). Degradation of Drosophila PIM regulates sister chromatid separation during mitosis. Genes Dev. *14*, 2192–2205.

Lengauer, C., Kinzler, K.W., and Vogelstein, B. (1997). Genetic instability in colorectal cancers. Nature *386*, 623–627.

Lengauer, C., Kinzler, K.W., and Vogelstein, B. (1998). Genetic instabilities in human cancers. Nature *396*, 643–649.

Li, Y., and Benezra, R. (1996). Identification of a human mitotic checkpoint gene: hsMAD2. Science *274*, 246–248.

Loeb, L.A. (1991). Mutator phenotype may be required for multistage carcinogenesis. Cancer Res. *51*, 3075–3079.

Losada, A., Hirano, M., and Hirano, T. (1998). Identification of Xenopus SMC protein complexes required for sister chromatid cohesion. Genes Dev. *14*, 1986–1997.

Martinez-Exposito, M.J., Kaplan, K.B., Copeland, J., and Sorger, P.K. (1999). Retention of the BUB3 checkpoint protein on lagging chromosomes. Proc. Natl. Acad. Sci. USA *96*, 8493–8498.

Masramon, L., Ribas, M., Cifuentes, P., Arribas, R., Garcia, F., Egozcue, J., Peinado, M.A., and Miro, R. (2000). Cytogenetic characterization of two colon cell lines by using conventional G-banding, comparative genomic hybridization, and whole chromosome painting. Cancer Genet. Cytogenet. *121*, 17–21.

Michel, L.S., Liberal, V., Chatterjee, A., Kirchwegger, R., Pasche, B., Gerald, W., Dobles, M., Sorger, P.K., Murty, V.V., and Benezra, R. (2001). *MAD2* haplo-insufficiency causes premature anaphase and chromosomal instability in mammalian cells. Nature *409*, 355–359.

Morgan, D.O. (1999). Regulation of the APC and the exit from mitosis. Nat. Cell Biol. *1*, E47–E53.

Nasmyth, K., Peters, J.M., and Uhlmann, F. (2000). Splitting the chromosome: cutting the ties that bind sister chromatids. Science *288*, 1379–1385.

Peters, J.M. (1999). Subunits and substrates of the anaphase-promoting complex. Exp. Cell Res. *248*, 339–349.

Rhee, I., Jair, K.W., Yen, R.W., Lengauer, C., Herman, J.G., Kinzler, K.W., Vogelstein, B., Baylin, S.B., and Schuebel, K.E. (2000). CpG methylation is maintained in human cancer cells lacking DNMT1. Nature *404*, 1003–1007.

Saez, C., Japon, M.A., Ramos-Morales, F., Romero, F., Segura, D.I., Tortolero, M., and Pintor-Toro, J.A. (1999). hpttg is over-expressed in pituitary adenomas and other primary epithelial neoplasias. Oncogene *18*, 5473–5476.

Speicher, M.R., Gwyn Ballard, S., and Ward, D.C. (1996). Karyotyping human chromosomes by combinatorial multi-fluor FISH. Nat. Genet. *12*, 368–375.

Stennicke, H.R., and Salvesen, G.S. (2000). Caspases—controlling intracellular signals by protease zymogen activation. Biochim. Biophys. Acta *1477*, 299–306.

Stratmann, R., and Lehner, C.F. (1996). Separation of sister chromatids in mitosis requires the Drosophila pimples product, a protein degraded after the metaphase/anaphase transition. Cell *84*, 25–35.

Sumara, I., Vorlaufer, E., Gieffers, C., Peters, B.H., and Peters, J.-M.

(2000). Characterization of vertebrate cohesin complexes and their regulation in prophase. J. Cell Biol. *151*, 749–762.

Taylor, S.S., and McKeon, F. (1997). Kinetochore localization of murine Bub1 is required for normal mitotic timing and checkpoint response to spindle damage. Cell *89*, 727–735.

Taylor, S.S., Ha, E., and McKeon, F. (1998). The human homologue of Bub3 is required for kinetochore localization of Bub1 and a Mad3/Bub1-related protein kinase. J. Cell Biol. *142*, 1–11.

Uhlmann, F., Lottspeich, F., and Nasmyth, K. (1999). Sister-chromatid separation at anaphase onset is promoted by cleavage of the cohesin subunit Scc1. Nature *400*, 37–42.

Uhlmann, F., Wernic, D., Poupart, M.-A., Koonin, E.V., and Nasmyth, K. (2000). Cleavage of cohesin by the CD clan protease separin triggers anaphase in yeast. Cell *103*, 375–386.

Waizenegger, I.C., Hauf, S., Meinke, A., and Peters, J.M. (2000). Two distinct pathways remove mammalian cohesin complexes from chromosome arms in prophase and from centromeres in anaphase. Cell *103*, 399–410.

Waldman, T., Lengauer, C., Kinzler, K.W., and Vogelstein, B. (1996). Uncoupling of S phase and mitosis induced by anticancer agents in cells lacking p21. Nature *381*, 713–716.

Yamamoto, A., Guacci, V., and Koshland, D. (1996a). Pds1p, an inhibitor of anaphase in budding yeast, plays a critical role in the APC and checkpoint pathway(s). J. Cell Biol. *133*, 99–110.

Yamamoto, A., Guacci, V., and Koshland, D. (1996b). Pds1p is required for faithful execution of anaphase in the yeast, Saccharomyces cerevisiae. J. Cell Biol. *133*, 85–97.

Yanagida, M. (2000). Cell cycle mechanisms of sister chromatid separation; roles of Cut1/separin and Cut2/securin. Genes Cells *5*, 1–8.

Zou, H., McGarry, T.J., Bernal, T., and Kirschner, M.W. (1999). Identification of a vertebrate sister-chromatid separation inhibitor involved in transformation and tumorigenesis. Science *285*, 418–422.